Nephrol Dial Transplant (2006) 21: 299–313
doi:10.1093/ndt/gfi210
Advance Access publication 1 November 2005

Nephrology Dialysis Transplantation

Original Article

Role of receptor for advanced glycation end-products and signalling events in advanced glycation end-product-induced monocyte chemoattractant protein-1 expression in differentiated mouse podocytes

Leyi Gu[1,2], Shinji Hagiwara[1], Qiuling Fan[1], Mitsuo Tanimoto[1], Mami Kobata[1], Michifumi Yamashita[1], Tomohito Nishitani[1], Tomohito Gohda[1], Zhaohui Ni[2], Jiaqi Qian[2], Satoshi Horikoshi[1] and Yasuhiko Tomino[1]

[1]Division of Nephrology, Department of Internal Medicine, Juntendo University School of Medicine, Tokyo, Japan and [2]Division of Nephrology, Shanghai Second Medical University affiliated Renji Hospital, Shanghai, China

Abstract

Background. Upregulation of local monocyte chemoattractant protein-1 (MCP-1) production is involved in glomerular damage through macrophage recruitment and activation in diabetic nephropathy. Treatment of db/db mice with soluble receptor for advanced glycation end-products (RAGE) prevented recruitment of macrophages to the glomeruli and reduced albuminuria, suggesting that binding of ligands and RAGE may be involved in MCP-1 expression. Therefore, we investigated the role of advanced glycation end-products (AGEs) in MCP-1 production by podocytes and signalling events after RAGE activation.

Methods. MCP-1 gene and protein expression were examined by using reverse transcription–polymerase chain reaction and enzyme-linked immunosorbent assay in differentiated mouse podocytes. Dichlorofluorescein-sensitive intracellular reactive oxygen species (ROS) generation was measured by confocal microscopy. RAGE, phosphorylation of mitogen-activated protein kinases, nuclear factor (NF)-κB, c-Jun and Sp1 were studied using western blotting and immunocytochemistry.

Results. Both differentiated and undifferentiated podocytes expressed RAGE. MCP-1 was induced by AGEs and carboxymethyllysine (CML) in a time-dependent and dose-dependent manner in differentiated podocytes. Neutralizing antibody for RAGE suppressed AGE- and CML-induced MCP-1 production. AGEs and CML rapidly generated intracellular ROS in podocytes. Blocking of ROS by using *N*-acetyl-L-cysteine abolished CML and H_2O_2-induced MCP-1 expression. Phosphorylated extracellular signal-regulated kinase (ERK) was found in podocytes incubated with CML and was prevented by *N*-acetyl-L-cysteine or 7′-amino 4 [trifluoromethyl]. PD98059, an inhibitor of ERK, partially prevented CML-induced MCP-1 gene expression. NF-κB and Sp1 were translocated into the nucleus after podocytes were incubated with CML for 60 min. Parthenolide and mithramycin A, inhibitors of NF-κB and Sp1, respectively, abolished CML-induced MCP-1 gene expression in a dose-dependent manner.

Conclusions. These results suggest that AGEs and CML induce MCP-1 expression in podocytes through activation of RAGE and generation of intracellular ROS. NF-κB and Sp1 regulate MCP-1 gene transcription.

Keywords: AGE; ERK; MCP-1; podocyte; RAGE; ROS

Introduction

Monocyte chemoattractant protein-1 (MCP-1) is a member of the C-C chemokine family regulating macrophage recruitment and is upregulated in many renal diseases [1] including diabetic nephropathy [2]. Studies using human biopsy materials and animal models have shown the presence of macrophage accumulation and MCP-1 expression in diabetic glomeruli, suggesting that MCP-1 may play an important role in the development of diabetic glomerular damage and glomerulosclerosis [3]. Previous studies showed that high glucose and glycated albumin

Correspondence and offprint requests to: Dr Yasuhiko Tomino. Division of Nephrology, Department of Internal Medicine, Juntendo University School of Medicine, Tokyo, Japan. Email: yasu@med.juntendo.ac.jp

induce MCP-1 production in cultured mesangial cells [4,5]. However, more recent research found that mRNA expression of MCP-1 appeared to be predominantly localized in podocytes in diabetic glomeruli [3]. We still did not know what induces MCP-1 production by podocytes. The intracellular mechanisms of MCP-1 upregulation in podocytes also remained unclear. Treating db/db mice with soluble receptor for advanced glycation end-products (RAGE) prevented recruitment of macrophages to the glomeruli, suggesting that ligand RAGE may play a key role in MCP-1 production in podocytes [6].

Expression of RAGE is enhanced in human diabetic kidney. Specifically, in glomeruli, RAGE is expressed at the base of podocytes, but not to any appreciable degree in mesangial or endothelial cells [7]. RAGE, a multiligand member of the immunoglobulin superfamily [8,9], engages ligands, AGEs and members of the S100/calgranulin family [10], and is implicated in expression of the receptor itself. Amplifies the pro-inflammatory response leading to diabetic complications and inflammation by a receptor-dependent mechanism [6,10–12]. These responses are dependent on RAGE-mediated signals and gene expression. It has been shown that RAGE ligation with its ligands results in the activation of multiple signalling pathways in different lines of cells [13–17]. However, little is known about how ligands, after ligation with RAGE, signal the podocytes involved in diabetic injury through macrophage migration and activation.

In the present study, we clarified the effects of AGEs as well as carboxymethyllysine (CML), a special AGE, on expression of MCP-1 in differentiated mouse podocytes and investigated the CML–RAGE signalling cascade in podocytes.

Subjects and methods

Reagents

S100 protein, 7′-amino 4 [trifluoromethyl] (AFC), wortmannin, LY333531, aminoguanidine hemisulfate, calphostin, parthenolide and mithramycin A were purchased from Sigma-Aldrich (St Louis, MO). Dimethylsulfoxide (DMSO), PD98059, *N*-acetyl-L-cysteine (NAC), diethylenetriaminepentoacetic acid (DTPA), sodium cyanoborohydride ($NaCNBH_3$) and H_2O_2 were purchased from Wako Co., Ltd (Osaka, Japan). SB203580 and SP600125 were purchased from Alexis Biochemicals Co. (San Diego, CA).

Preparation of AGE protein and CML–BSA

AGEs were prepared as described previously [18]. Briefly, bovine serum albumin (BSA) was incubated with 0.5 M D-glucose and 5 mM DTPA in phosphate buffer at 37°C for 8 weeks. Control BSA was prepared under the same conditions without glucose. In parallel preparations, aminoguanidine at 250 mM was added as an inhibitor of the formation of products of non-enzymatic glycation. The preparations were dialysed extensively against phosphate-buffered saline (PBS). AGE content was determinated by measuring emission at 420 nm on excitation at 340 nm using a fluorescence spectrophotometer (F-4500, Hitachi, Japan) at a protein concentration of 1 mg/ml. The fluorescence value of BSA, AGE, and AGE plus aminoguanidine is 16.67, 161.95 and 18.30 units, respectively.

CML–BSA was prepared as described elsewhere [18]. Briefly, 50 mg/ml of BSA was incubated at 37°C for 24 h with 45 mM glyoxylic acid and 150 mM $NaCNBH_3$ in phosphate buffer, followed by dialysis against PBS. The extent of lysine modification was determined by the trinitro benzene sulfonic acid (TNBS) method, and the modification (%) of AGE and CML was 51.86 and 55.17%, respectively. The protein concentration was determined by BCA assay (Pierce Inc., Rockford, IL). Endotoxin in the preparations was tested using an Endospecy ES-20S system and the level of endotoxin in all protein preparations was <10 pg/ml.

Cell culture of podocytes

The conditionally immortalized mouse podocytes, which were a gift from Dr Peter Mundel, were cultured as described elsewhere [19]. In brief, podocytes were maintained in RPMI 1640 medium supplemented with 10% fetal calf serum (FCS; Gibco-BRL, Gaithersburg, MD) and 10 IU/ml recombinant mouse γ-interferon (Pepro Tech EC Ltd, London) at 33°C (permissive conditions). To induce differentiation, podocytes were cultured at 37°C without γ-interferon (non-permissive conditions). After 8 days under non-permissive conditions, the majority of cells had an arborous shape and expressed synaptopodin. Differentiated podocytes were starved in Dulbecco's modified Eagle's medium (DMEM) containing 0.1% fetal calf serum (FCS) for 24 h. The cells were then treated with various reagents. All experiments were repeated at least three times in each indicated condition. Podocytes between passages 15 and 20 were used in all experiments.

Assay of intracellular ROS

Intracellular ROS production was measured by the method of Bass *et al.* [20], and modified for confocal microscopy [21]. In brief, podocytes were incubated in the dark for 30 min in DMEM without phenol red containing 10 μM 5-(and-6)-chloromethyl-2′,7′-dichlorodihydrofluorescein diacetate ($CM\text{-}H_2DCFDA$; Molecular Probes Inc., Eugene, OR). Culture plates were transferred to a Nikon TE300 (Nikon Co., Tokyo, Japan) inverted microscope with a BIO RAD MRC1024 confocal attachment. The ROS generation was detected as a result of the oxidation of DCFH (excitation, 488 nm; emission, 515–540 nm). Fluorescence images were recorded using a confocal attachment. Thereafter, cells were detached from the culture dish using trypsin. Fluorescence values were determined by measuring emission at 519 nm for excitation at 488 nm using a fluorescence spectrophotometer (F-4500, Hitachi, Japan). The values were normalized to the total protein content.

RNA preparation and RT–PCR

Total RNA was isolated from podocytes using TRIZOL reagent (Life Technologies Inc., Grand Island, NY) according to the manufacturer's instructions. A 1 μg aliquot of total RNA was reverse-transcribed using oligo(dT) primers (Life Technologies, Rockville, MD) and reverse transcriptase,

Superscript II (Life Technologies). The product was denatured and amplified in the GeneAmp PCR System 9600 (Perkin-Elmer, Norwalk, CT). Aliquots of cDNA were amplified with *Taq* polymerase and the following specific primers: MCP-1 sense, 5′-TGTCT GGACC CATTC CTTCT-3′ and antisense, 5′-ACCAGCAAGATGATCCCAAT-3′; GAPDH, sense, 5′-GGAGACAACCTGGTCCTCAG-3′ and antisense, 5′-ACCCAGAAGACTGTGGATGG-3′; RAGE sense, 5′-CAGGGTCACAGAAACCGG-3′ and antisense, 5′-ATTCA GCTCT GCACG TTCCT-3′. One cycle of 94°C for 5 min, and 25 cycles of 94°C for 30 s, 56°C for 30 s and 72°C for 60 s were used for MCP-1 and GAPDH; it had been demonstrated in preliminary research that the amplification proceeded linearly in the range from 23 to 29 cycles. One cycle of 92°C for 5 min, and 35 cycles of 92°C for 30 s, 60°C for 90 s and 72°C for 60 s were used for RAGE. Polymerase chain reaction products were electrophoresed on a 2% agarose gel containing ethidium bromide. The OD was measured by a BIO RAD 5000 image system and arbitrarily compared before treatment. PCRs resulted in the amplification of a single product of the predicted size for MCP-1 (140 bp), GAPDH (300 bp) and RAGE (213 bp). We chose GAPDH as a housekeeping gene and used its gene product to normalize RT–PCR data.

Measurements of MCP-1 by ELISA

To quantify the level of MCP-1 protein under various experimental conditions, the level of supernatant MCP-1 was measured using a solid phase quantitative sandwich enzyme-linked immunosorbent assay (ELISA) kit for MCP-1 (BD Biosciences, San Diego, CA) that was specific for mouse MCP-1 and sensitive to 10 pg/ml. The concentration in culture supernatant was normalized to the total protein content.

Immunocytochemistry staining

Podocytes were fixed with 3.7% formaldehyde and 2% sucrose/PBS for 10 min, permeabilized with 0.5 or 0.01% Triton X-100 for 5 min, and blocked with blocking solution (2% BSA, 2% FCS, 0.2% fish gelatin in PBS). Cells were incubated with primary antibodies, and subsequent recognition was with Alexa Fluor® 488-conjugated or fluorescein isothiocyanate (FITC)-conjugated secondary antibodies (1:500, Molecular Probes Inc., Eugene, OR). Cells were mounted in Prolong antifade mounting media. Fluorescence images were recorded using a Nikon TE300 inverted confocal microscope with excitation at 488 nm and long-pass detection at 519 nm. The primary antibodies used in immunocytochemistry were as follows: mouse anti-human phospho-c-Jun antibody (1 μg/ml), rabbit anti-human NF-κB P65 antibody (1:500) and rabbit anti-human Sp1 antibody (2.5 μg/ml).

Preparation of nuclear proteins

Nuclear proteins were prepared as described previously [22]. In brief, podocytes were scraped into cold PBS. Cells were pelleted by 10 s centrifugation at 15 000 r.p.m. and resuspended in buffer A [10 mM HEPES-KOH pH 7.9 at 4°C, 1.5 mM $MgCl_2$, 10 mM KCl, 0.5 mM dithiothreitol (DTT) and 0.2 mM phenylmethylsulfonyl fluoride (PMSF)], incubated on ice and centrifuged at 15 000 r.p.m. in a table-top centrifuge. The nuclear pellets were resuspended in 40–100 μl of buffer B (20 mM HEPES-KOH, 1.5 mM $MgCl_2$, 420 mM NaCl, 25% glycerol, 0.2 mM EDTA, 0.5 mM DTT and 0.2 mM PMSF), incubated on ice for 20 min, and centrifuged for 2 min as above. The supernatant fraction containing nuclear proteins was immediately frozen at −80°C.

Immunoblot analyses

SDS–PAGE and immunoblot analyses were carried out according to standard protocols and visualized using enhanced chemiluminescence (ECL) immunoblot detection kits (Amersham Pharmacia Biotech, Little Chalfont, Buckinghamshire, UK). The primary antibodies used in this study were as follows: mouse anti-human phospho-ERK1/2 antibody (1 μg/ml), rabbit anti-human ERK1/2 antibody (1:1000), rabbit anti-human phosphor-p38 mitogen-activated protein (MAP) kinase antibody (1:1000), rabbit anti-human phosphor-SAPK antibody (1:1000), mouse anti-human phospho-c-Jun antibody (0.2 μg/ml) (Cell Signaling Technology, Inc., Beverly, MA), rabbit anti-human NF-κB P65 antibody (1:3000), goat anti-human RAGE antibody (1:1000), mouse anti-chicken actin antibody (1:1000) (Chemicon, Inc., Temecula, CA) and rabbit anti-human Sp1 antibody (1 μg/ml) (Upstate, NY). Horseradish peroxidase (HRP)-conjugated secondary antibodies (Jackson-Immunoresearch Laboratonies, Inc., West Grove, PA) were used in this study. The OD was measured by a BIO RAD 5000 image system and arbitrarily compared before treatment.

Statistical analyses

All results are expressed as the mean ± SEM. Statistical analyses were performed by SAS 6.04. Analysis of variance (ANOVA) with DUNCAN analysis and the DUNNETT test was used to assess differences between multiple groups. $P < 0.05$ was considered as a statistically significant difference.

Results

Both undifferentiated and differentiated podocytes expressed RAGE

As shown in Figure 1, the expression of RAGE mRNA (Figure 1A) and protein (Figure 1B) was detected in both differentiated and undifferentiated podocytes.

RAGE-dependent AGE-, CML- and S100-induced MCP-1 expression in podocytes

MCP-1 mRNA was increased to 156.7 ± 17.1, 193.2 ± 26.4 and 242.1 ± 45.7% (P ± 0.05) when podocytes were stimulated using 200 mg/ml, 500 mg/ml and 1000 mg/ml CML, respectively. AGE and S100, another ligand for RAGE, had a similar effect.

Both AGE- and CML-induced expression of MCP-1 mRNA was abolished completely by the neutralizing antibodies to RAGE (RAGE-Ab, Chemicon Inc., Temecula, CA) [23]. Non-immune IgG was not able

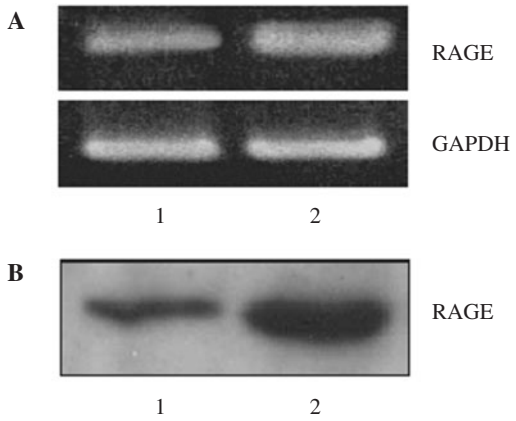

Fig. 1. Both undifferentiated and differentiated podocytes express RAGE. (**A**) RT–PCR was performed with total RNA isolated from undifferentiated and differentiated podocytes. (**B**) Whole cell lysates were prepared, normalized to equal protein concentration and analysed by western blotting using antibodies to RAGE. Llne 1, undifferentiated podocytes; lane 2, differentiated podocytes.

to reduce AGE- and CML-induced expression of MCP-1 mRNA (Figure 3A). As shown in Figure 3B, AGE-, CML- and S100-incubated podocytes produced more MCP-1 protein than BSA after 8 h of incubation, with a concentration of 5.88 ± 0.96, 6.33 ± 0.70 and 26.30 ± 4.17 *vs* 3.21 ± 0.57 pg/mg, respectively ($P < 0.05$). The protein concentrations of MCP-1 were elevated after 24 h ($P < 0.001$). RAGE-Ab abolished these effects completely. The concentration of MCP-1 in the supernatant was 3.70 ± 0.06, 3.04 ± 0.08 and 3.40 ± 0.45 pg/mg in the podocytes which were incubated with AGE, CML and S100, respectively, in the presence of RAGE-Ab. However, non-immune IgG did not inhibit the MCP-1 protein production.

Role of ROS in AGE- and CML-induced MCP-1 mRNA expression in podocytes

In the inactive state, basal ROS were observed in the nucleus of podocytes. Intracellular ROS were detected in cytoplasm and nuclei when the cells were incubated

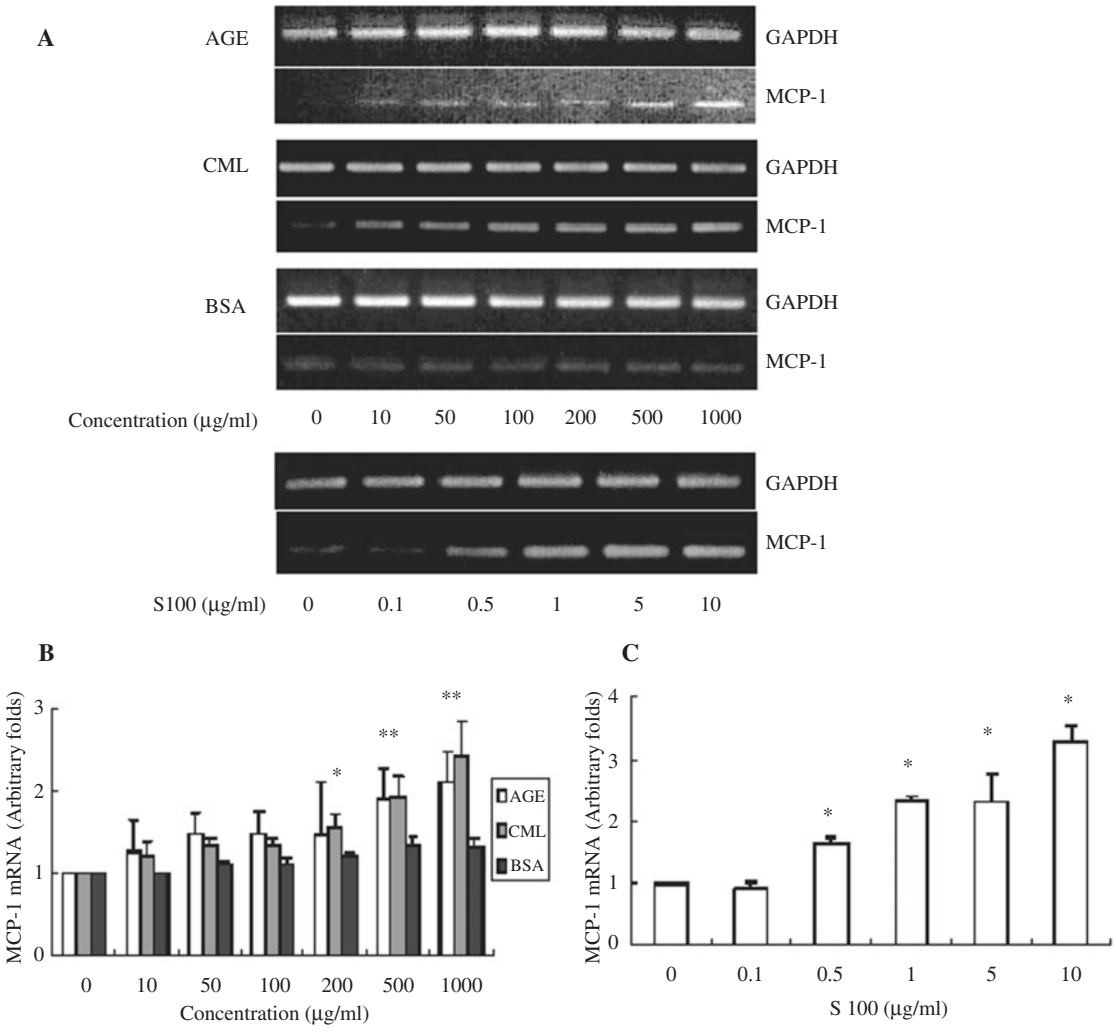

Fig. 2. AGE, CML and S100 induced MCP-1 mRNA expression in a dose-dependent manner in podocytes. (**A**) Podocytes were treated with or without various concentrations of AGE, CML, BSA (10–1000 μg/ml) and S100 (0.1–10 μg/ml) for 4 h, then total RNA was extracted for analysis by RT–PCR, using GAPDH as internal control. (**B** and **C**) Bar graph of data obtained from four independent experiments expressed as fold over the respective control. *$P < 0.05$ compared with the corresponding reagent at 0 μg/ml.

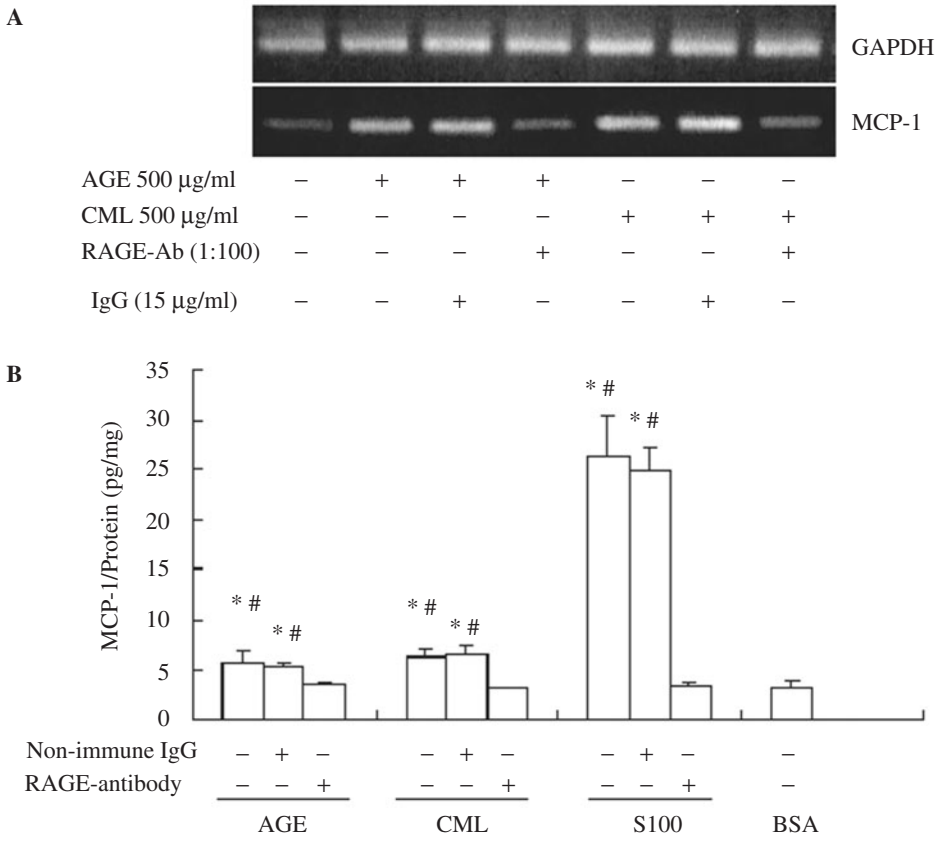

Fig. 3. RAGE dependent AGE-, CML- and S100-induced MCP-1 mRNA and protein production in podocytes. (**A**) Podocytes were treated with AGE or CML in the presence or absence of antibody for RAGE (RAGE-Ab) or non-immune IgG. Then RNA was extracted for RT–PCR. (**B**) Podocytes incubated with 1 μg/ml of S100, or 500 μg/ml of AGE or CML in the presence or absence of RAGE-Ab and non-immune IgG for 8 h. All data are from at least three independent experiments. $^{*}P < 0.05$ compared with BSA incubation. $^{\#}P < 0.05$ compared with the corresponding reagents incubated in the presence of RAGE-Ab.

with AGE and CML for 30 min (Figure 4A and B). Both basal ROS and induced ROS were inhibited by pre-treatment with NAC. CML also lost the ability to induce intracellular ROS generation in the presence of RAGE-Ab, but not non-immune IgG, as shown in Figure 4C and D. Exogenous H_2O_2 induced maximum MCP-1 mRNA expression after 2 h of incubation. This expression increased to 154.5 ± 34.4 and $183.4 \pm 33.5\%$ ($P < 0.05$) in podocytes treated with 10 and 100 μM H_2O_2, respectively, and was abolished by the presence of NAC, as shown in Figure 5.

Effect of CML on the podocyte MAP kinase family

As shown in Figure 6A and B, phosphorylated ERK1/2 was found after 10 min of incubation and maximal activation was reached after 30 min of stimulation. However, we were unable to detect any activation of p38 MAP kinase and SAPK under CML treatment. Pre-treating podocytes with a ROS inhibitor (NAC), Ras inhibitor (AFC) and MEK inhibitor (PD98059), but not a protein kinase C (PKC) inhibitor (calphostin) or phosphatidylinositol-3 kinase (PI3K) inhibitor (wortmannin), abolished the ERK1/2 activation. These results suggested that the activation of ERK1/2 was dependent on ROS and/or Ras-MEK (Figure 6C).

As summarized in Figure 7, CML increased MCP-1 mRNA expression to $192.0 \pm 40.0\%$ ($P < 0.05$). Pre-treatment with NAC and AFC completely prevented CML-induced MCP-1 expression, whereas PD98059 only partially inhibited the increase. Therefore, part of the effect of CML on MCP-1 expression may be not via an ERK1/2 pathway. We did not demonstrate any effect of calphostin, LY333531, wortmannin, SB203580 or SP600125 on MCP-1 mRNA expression.

Activation of Sp1 and NF-κB is involved in the regulation of MCP-1 gene transcription

As shown in Figure 8A, we found that Sp1 protein started to accumulate in the nucleus from 20 min of CML incubation and remained elevated until 120 min. However, the P65 subunit of NF-κB was concentrated in the nucleus from 60 min of incubation (Figure 8B). Phosphorylated c-Jun, an activator of AP-1, could not be detected until 2 h of incubation (Figure 8C). In immunocytochemical staining, shown in Figure 8E, NF-κB and Sp1 were found in the cytoplasm

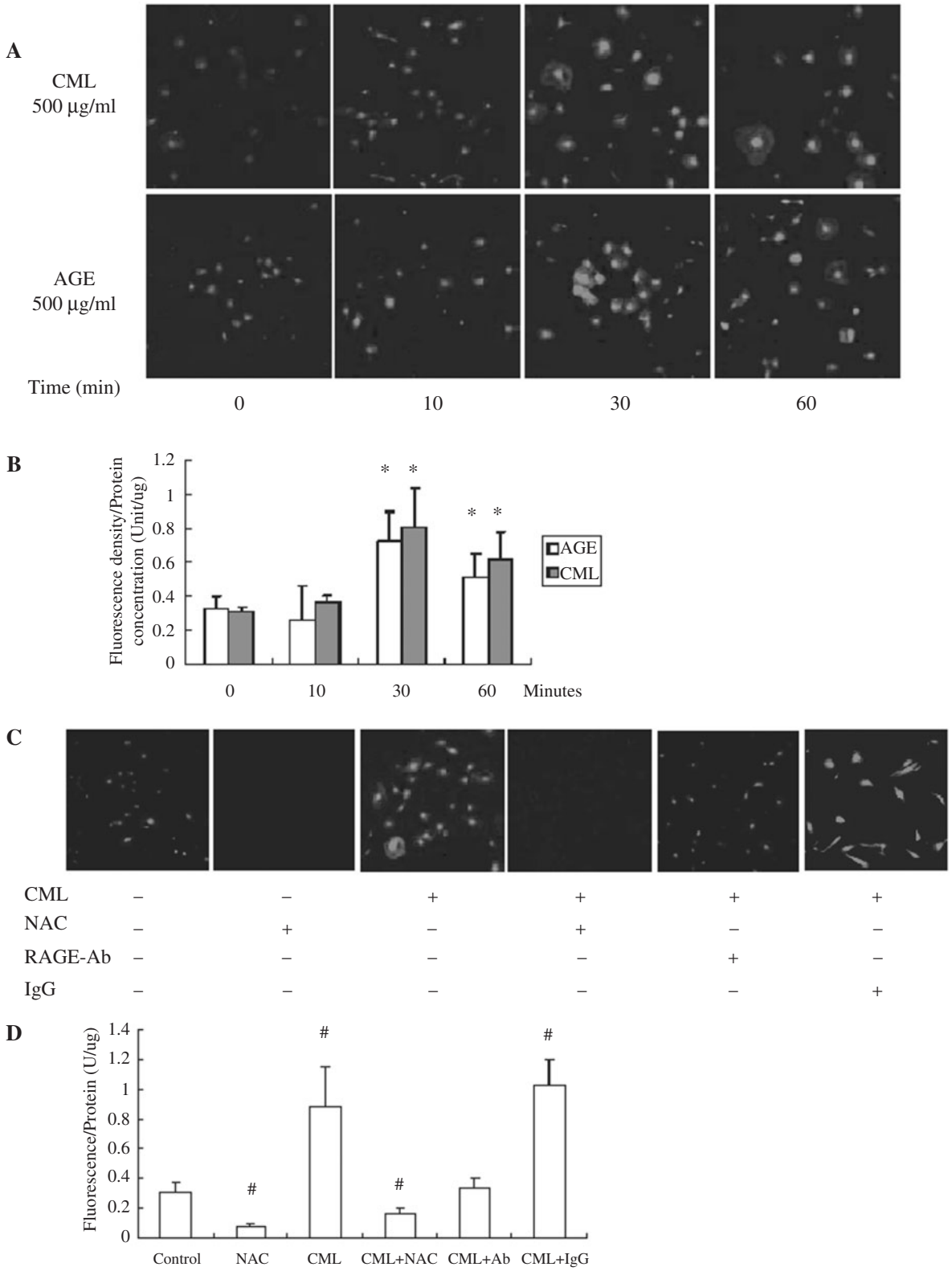

Fig. 4. Both AGE and CML induce intracellular ROS generation in podocytes. The specificity of 2′-7′ dichlorofluorescein (DCF)-sensitive ROS was visualized by confocal microscopy. (**A**) Podocytes were incubated with AGE or CML for the indicated time (0–60 min). (**B**) A bar graph of data obtained from four independent experiments. (**C**) After pre-treatment by 30 mM NAC, RAGE-Ab or non-immune IgG, podocytes were incubated with 500 μg/ml CML for 60 min. Images were recorded by confocal microscopy (magnification ×100). (**D**) A bar graph of data obtained from three to four independent experiments. $^{*}P < 0.05$ compared with 0 min; $^{\#}P < 0.05$ compared with control.

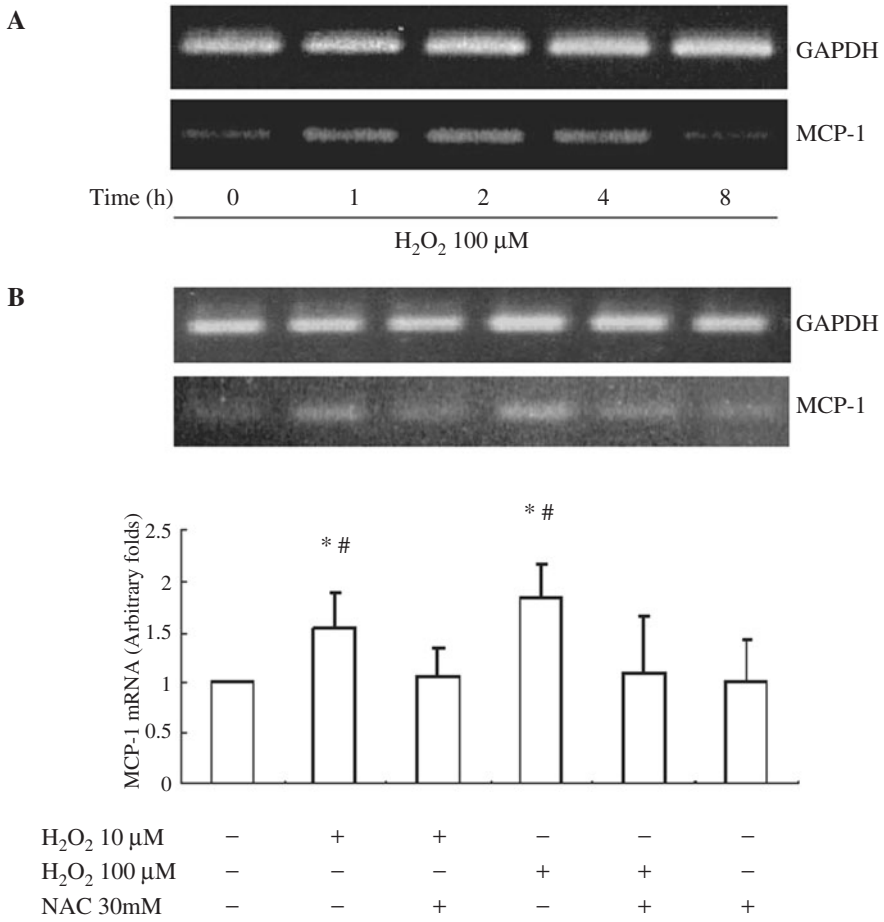

Fig. 5. Effect of H_2O_2 on MCP-1 mRNA expression in podocytes. (**A**) Podocytes were treated with 100 μM H_2O_2 for the indicated periods, then RNA was isolated for RT–PCR. (**B**) Podocytes were treated with H_2O_2 in the presence or absence of 30 mM NAC for 2 h, then total RNA was extracted for analysis by RT–PCR. Bar graphs of data were prepared from three independent experiments expressed as fold change over control. $^{*}P < 0.05$ compared with control; $^{\#}P < 0.05$ compared with incubation with corresponding reagents in the presence of NAC.

of podocytes before treatment with CML; however, after incubation with CML for 60 min, NF-κB translocated to the nucleus. Sp1 could be detected only in some podocyte nuclei. We did not find phosphorylated c-Jun expression in activated and inactivated podocytes.

As shown in Figure 9, mithramycin A suppressed CML-induced MCP-1 mRNA expression in a dose-dependent manner. Pre-treatment of podocytes with 1 μM mithramycin A, or 10 or 100 nM parthenolide abolished CML-induced MCP-1 gene transcription completely.

CML-induced NF-κB and Sp1 activation is dependent on ROS and p21Ras

NAC, AFC and PD98059 abolished NF-κB translocation into the nucleus (Figure 10). Unlike NF-κB, Sp1 could not be inhibited by MEK inhibitor even though AFC and NAC abolished the increase of Sp1 in the nuclei.

Discussion

In the present study, our data clearly suggested that AGE and CML stimulated MCP-1 mRNA and protein expression through RAGE and the ROS-dependent signalling pathway in differentiated mouse podocytes. Our data also demonstrated that CML-induced MCP-1 expression is regulated by NF-κB and Sp1.

Podocyte slit diaphragm-associated proteins play a central role in maintaining the size-selective barrier, and podocyte injury or activation contributes to macroproteinuria in diabetic nephropathy [23]. The urinary MCP-1 level is significantly elevated in diabetic nephropathy patients with macroproteinuria, and suppression of urinary MCP-1 improves diabetic nephropathy [2,24]. Recent studies showed that, in diabetic glomeruli, expression of MCP-1 mRNA appeared to be predominantly localized in podocytes [3]. This evidence suggests that MCP-1 is involved in development of diabetic nephropathy [25], and podocyte injury may contribute to MCP-1 production.

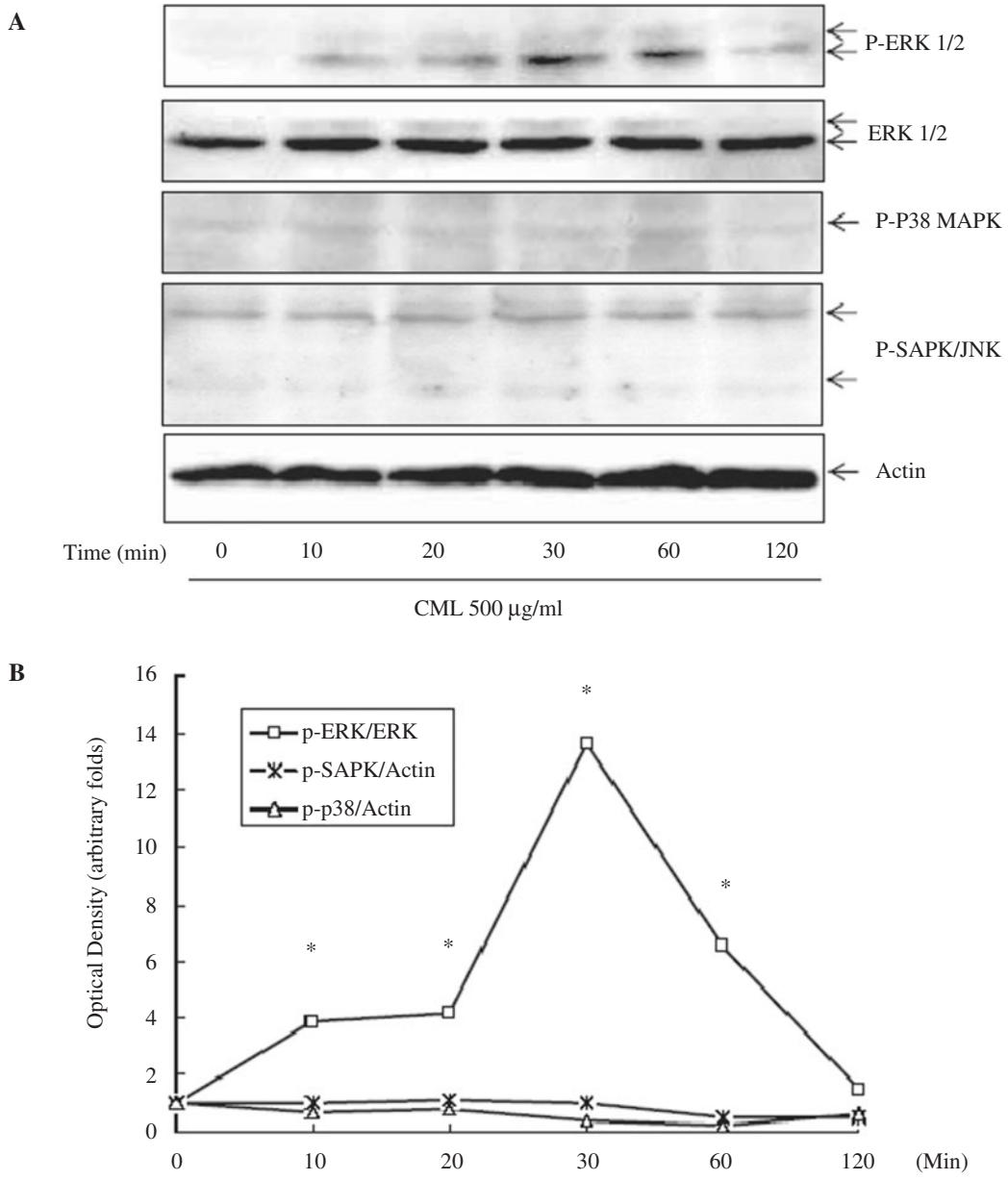

Fig. 6. Activation of ERK in CML-incubated podocytes. Cells were treated with CML for the indicated time. (**A**) A line graph of data was obtained from three independent experiments expressed as fold change over 0 min. (**B**) Podocytes were pre-treated with calphostin (100 nM, PKC inhibitor), AFC (50 μM, p21Ras inhibitor), LY333531 (25 nM, selective PKC-β inhibitor), wortmannin (100 nM, PI3K inhibitor), NAC (30 mM, ROS scavenger) and PD98059 (50 μM, MEK inhibitor) for 30 or 60 min, then incubated with 500 μg/ml of CML for 30 min. (**C**) Whole-cell lysates were prepared, normalized to equal protein concentration and analysed by western blotting using antibodies to phosphorylated ERK1/2 (P-ERK1/2), phosphorylated p38 MAP kinase (P-p38 MAPK), phosphorylated SAPK/JNK (P-SAPK/JNK) and normal ERK1/2 or actin as control. $^{*}P < 0.05$ compared with 0 min; $^{\#}P < 0.05$ compared with control; $^{\S}P < 0.05$ compared with CML-treated podocytes.

Our data provide direct evidence that both AGE and CML, which accumulate in the diabetic mesangium and glomerular basement membranes (GBM), induce MCP-1 expression in a time- and dose-dependent manner in podocytes. These results were coincident with the observations in animal studies. Treatment of db/db mice with sRAGE prevented macrophage migration to the glomeruli and inhibited vascular endothelial growth factor (VEGF) secretion from podocytes [6]. Since podocytes face the urinary space directly, MCP-1 produced by podocytes may not only mediate migration of macrophages into glomeruli, but can also be secreted into urine. Therefore, the elevated urinary MCP-1 was at least in part derived from activated podocytes, and the urinary level of MCP-1 in diabetic patients may reflect advancing

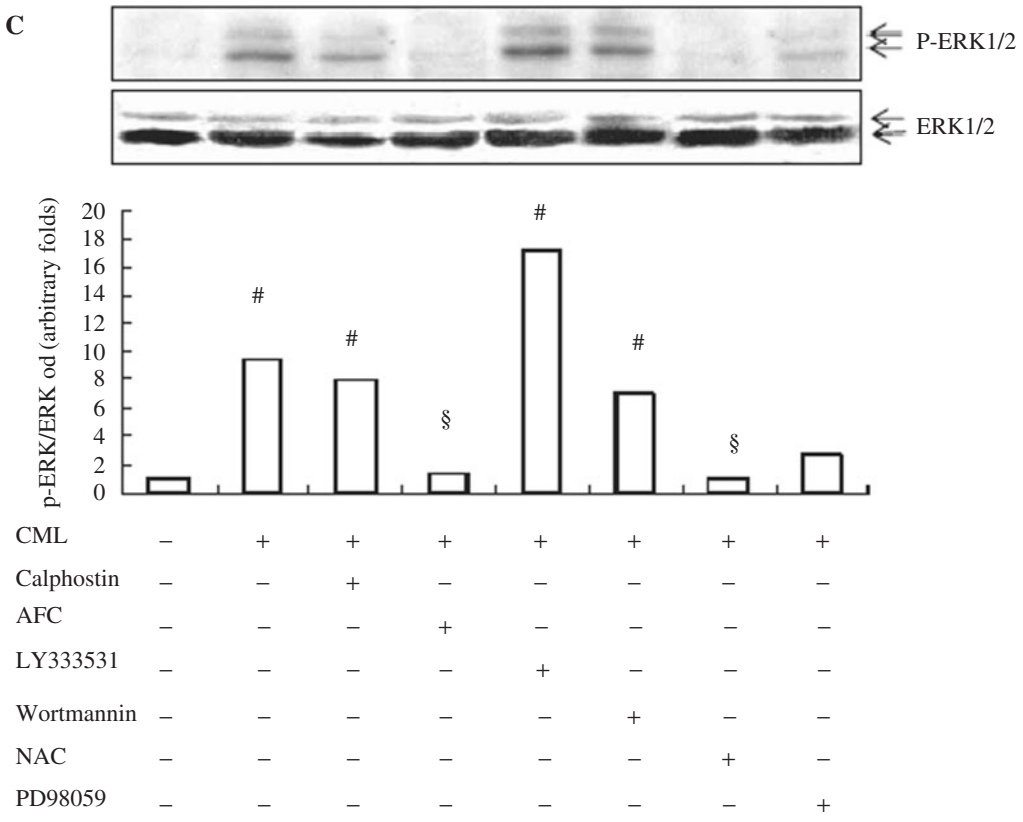

Fig. 6. Continued.

glomerular lesions and podocyte injury. It has been demonstrated that urinary MCP-1 activates tubular epithelial cells, leading to an increase in secretion of the proinflammatory cytokine interleukin-6 (IL-6) and the intercellular adhesion molecule-1 (ICAM-1) [26]. Thus, they trigger or aggravate tubular atrophy, interstitial infiltrates and inflammation.

In the present research, relatively high concentration of AGE and CML activated podocytes significantly. The concentration of glycated albumin in non-diabetic individuals is almost 350–400 μg/ml, which is increased >1.5-fold in diabetic subjects [22,27]. AGE and CML accumulate in GBM and mesangium in the diabetic environment, so the local concentration of AGE and CML is higher than the systemic concentration. The effects of a relatively high concentration of AGE and CML may occur *in vivo*. The fact that the physiological concentration of S100 activates podocytes also supports this idea. Neutralizing antibody for RAGE abolished AGE-, CML- and S100-induced MCP-1 production, indicating that the pathways of MCP-1 regulation in podocytes may be at least in part RAGE-dependent. Furthermore, accumulation of CML and upregulation of RAGE in podocytes were also observed in the sclerotic glomeruli of non-diabetic nephropathy [7,28], suggesting that RAGE binding with ligands activates podocytes and promotes the sclerosis of glomeruli. Recently, the expression of megalin, another AGE receptor which is involved in the uptake of proteins from extracellular sources, was identified in podocytes [29]. It is interesting to note the contribution of this endocytic receptor in the activation of podocytes.

ROS have been identified as signalling molecules for signal transduction of several receptors, including RAGE, in several lineages of cells. We found that AGE and CML can rapidly generate intracellular ROS dependent on RAGE activation in podocytes, and a ROS scavenger abolished CML- and H_2O_2-induced MCP-1 expression. ROS also induced granulocyte–macrophage colony-stimulating factor expression in podocytes [30]. These results suggest that ROS play a crucial role in recruitment of macrophages into glomuli. Not only do ROS play an important role in the activation of podocytes, but they also mediated puromycin aminonucleoside-induced injury of podocytes [31,32]. Thus, prevention of podocyte ROS generation presents a potential therapeutic target to protect against podocyte injury.

We could not detect activation of p38 MAP kinase and SAPK in podocytes treated with CML. Both p38 MAP kinase inhibitor and SAPK inhibitor failed to abolish CML-induced MCP-1 mRNA expression, demonstrating the ability of CML to stimulate MCP-1 expression through ERK, but not p38 MAP kinase or the SAPK signalling pathway. We could not

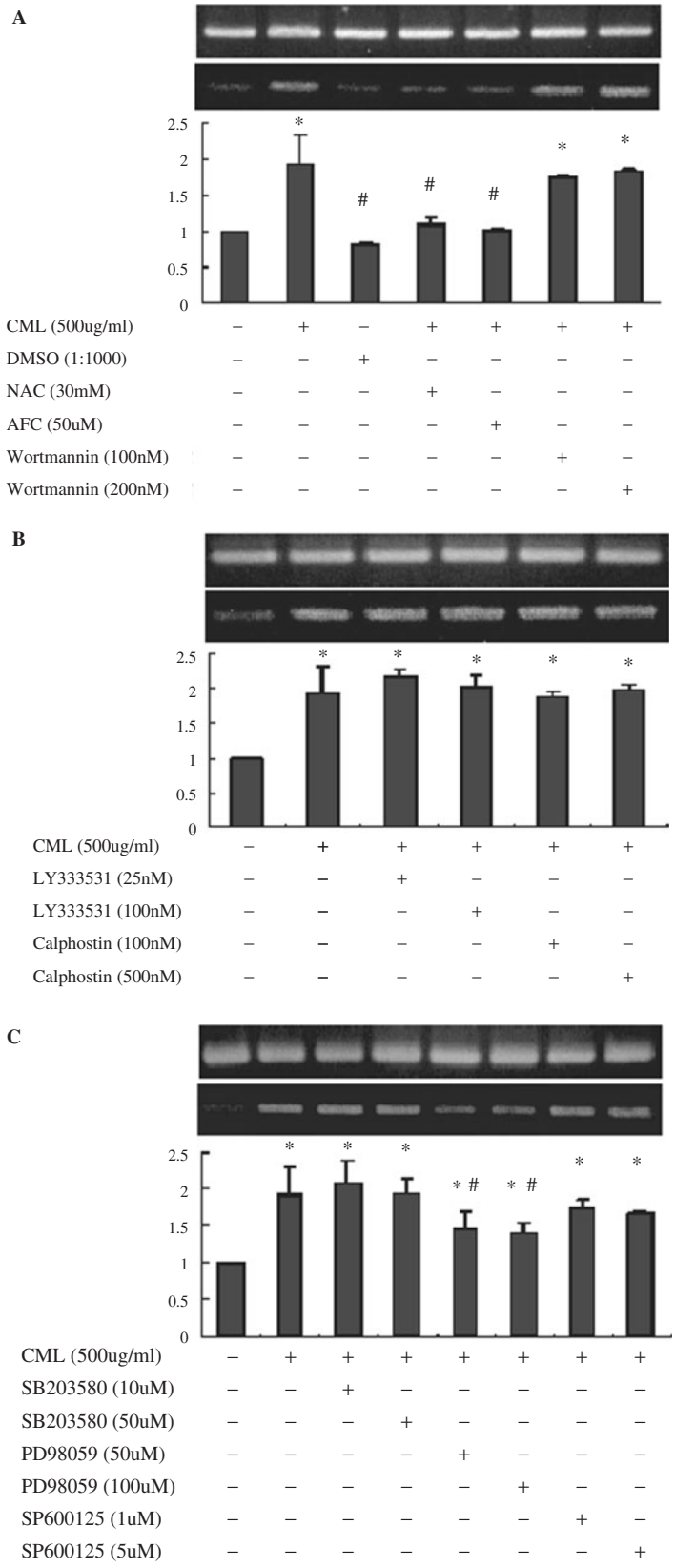

Fig. 7. Signalling pathway implicated in CML-induced MCP-1 expression. RT–PCR was performed with total RNA isolated from podocytes which were treated with 500 μg/ml CML for 4 h in the presence or absence of DMSO, NAC, AFC, wortmannin, LY333531, calphostin, SP600125, SB203580 and PD98059 using GAPDH as internal control. A bar graph of data was obtained from three independent experiments expressed as fold change over control. $^{*}P < 0.05$ compared with unincubated podocytes; $^{\#}P < 0.05$ compared with podocytes incubated with CML.

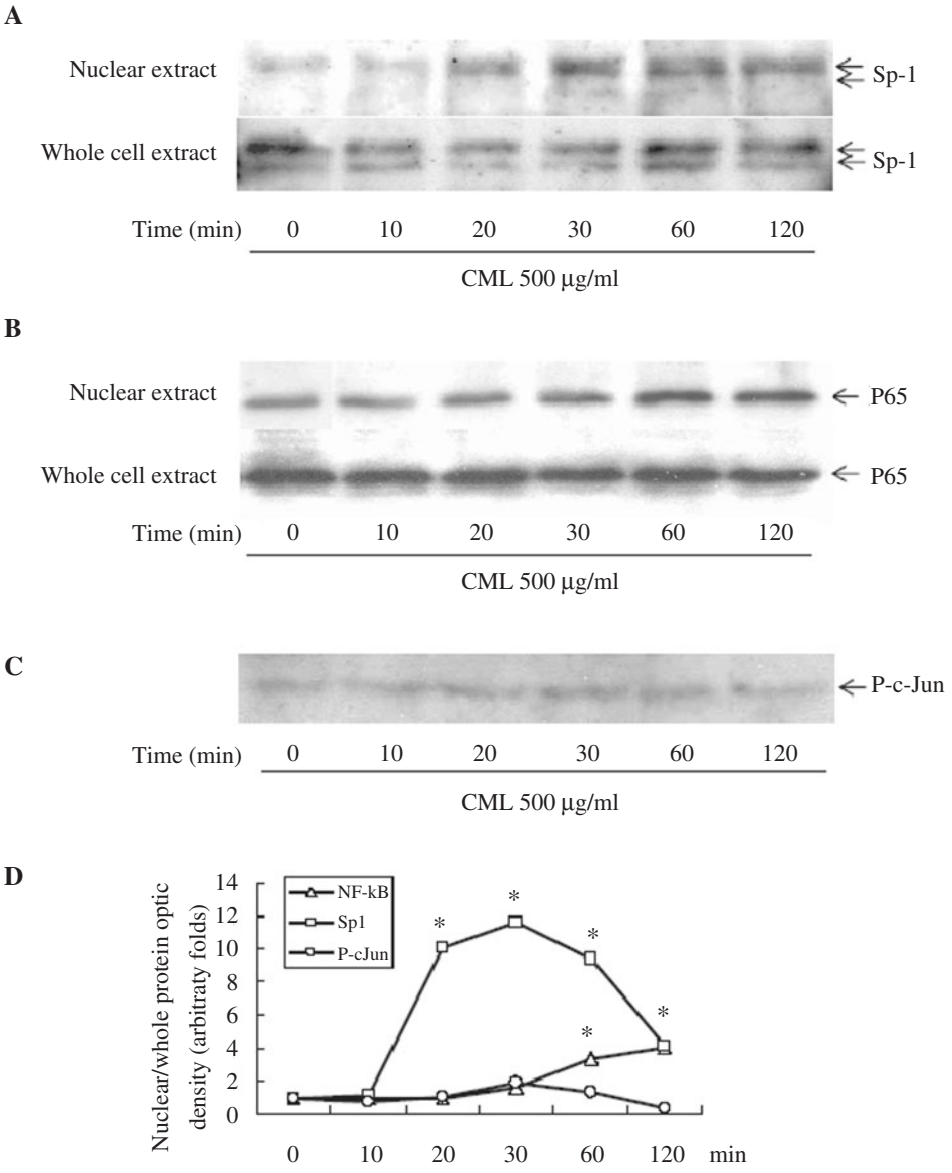

Fig. 8. Sp1 and NF-κB, but not c-Jun were activated by CML. Podocytes were treated with CML (500 μg/ml) for the indicated time (0–120 min). Nuclear protein and whole cell protein was collected using the method described in Materials and methods, then 5 μg of nuclear protein or whole cell protein was analysed by western blotting using antibodies to Sp1 (**A**), p65 (**B**) and phosphorylated c-Jun (P-c-Jun) (**C**). (**D**) A bar graph of data obtained from three independent experiments expressed as fold change over 0 min. (**E**) Podocytes were treated with or without CML for 60 min and immunocytochemical staining was performed. The arrowhead indicates weak nuclear staining of unstimulated podocytes and parts of stimulated cells. Increased nuclear staining was found in some stimulated cells (arrow), magnification ×200. *$P < 0.05$ compared with 0 min.

obtain any evidence that PI3K or PKC is involved in activation of transcription of MCP-1 mRNA, although recent studies demonstrated that PKC plays a key role in the regulation of MCP-1 gene expression, and activation by S100 in mesangial cells is dependent on PI3K [33]. Similarly to MAP kinases, activation of PI3K and PKC may be cell-specific reactions.

There are two regulatory regions containing NF-κB-, AP-1- and Sp1-binding sites, which have been identified at the promoter region of the mouse MCP-1 gene [34,35]. All of these transcription factors are important for regulation of MCP-1 gene transcription [35–37]. In mesangial cells and embryonic fibroblasts, NF-κB regulates only high glucose- or tumour necrosis factor (TNF)-α-induced MCP-1 expression [4]. Park *et al.* had demonstrated that NF-κB and AP-1 regulate TNF-α-induced MCP-1 expression in glomerular endothelial cells [36]. We observed that both p65 and Sp1, but not c-jun, were increased in nuclei by using

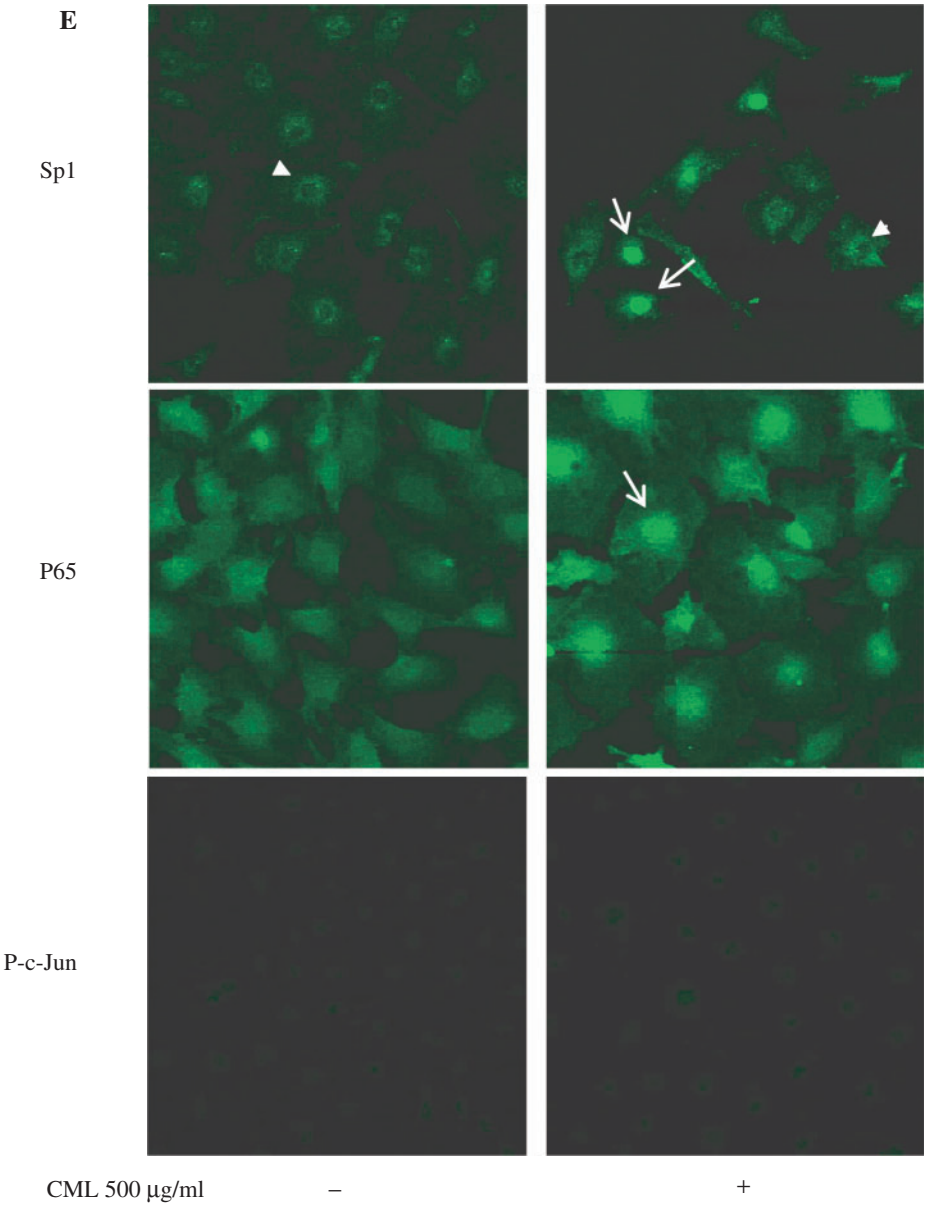

Fig. 8. Continued.

western blotting and immunocytochemistry. The inhibitors of NF-κB and Sp1 prevented CML-induced MCP-1 mRNA expression, suggesting that both are regulators of the gene of MCP-1 transcription. We also found that the p65 and Sp1 protein contents in the whole cell remained unchanged after incubation with CML. These data suggest that Sp1, like NF-κB, translocated into the nucleus. This hypothesis is supported by other observations. Keembiyehetty *et al.* found that there is positive Sp1 staining in nuclei and diffuse cytoplasmn patterns when Sp1 expression is decreased in the H-411E cell nucleus [38]. Zhang *et al.* showed that H_2O_2 induced Sp1 binding to DNA without any increase of Sp1 production in podocytes [39]. Sp1 is also involved in transforming growth factor (TGF)-β signal transduction [40,41]. It mediates the TGF-β-stimulated type IV collagen gene transcription [42], which is believed to be a central mediator of glomerulosclerosis. Sp1 activation by CML in the present study raises the question of whether Sp1 activation following CML–RAGE interaction mediates or amplifies the virulent effect of TGF-β in podocytes as the next step in our study. Mithramycin A dose dependently blocked MCP-1 mRNA expression, suggesting that Sp1 regulates MCP-1 gene transcription directly.

The results of Huttunen *et al.* and those of the present experiment indicated that AGE-induced NF-κB

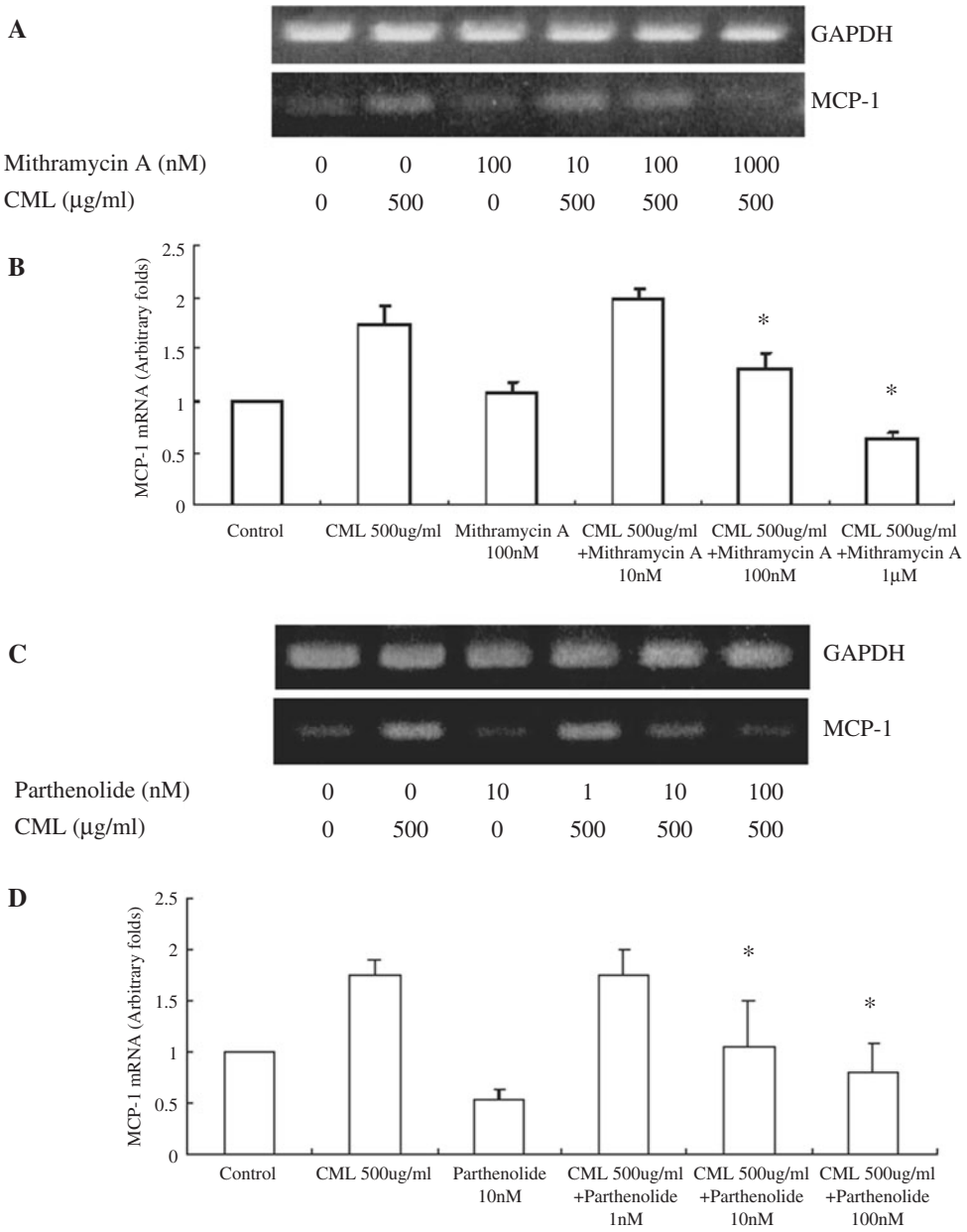

Fig. 9. Effects of mithramycin A and parthenolide on MCP-1 mRNA expression in podocytes. (**A**) Podocytes were pre-treated with the indicated concentration of mithramycin A for 24 h. After incubation of podocytes with CML, RNA was isolated for RT–PCR and GAPDH was used as the internal control. (**B**) A bar graph of data obtained from three independent experiments expressed as fold change over control. (**C**) Cells were pre-treated with various concentration of parthenolide for 1 h. After incubation of CML, RNA was extracted from podocytes for RT–PCR. (**D**) A bar graph showing the mean ± SE from three independent experiments, expressed as fold change over control. $*P < 0.05$ compared with cells incubated with CML.

activation is dependent on ROS–p21Ras–ERK [14]. The upstream signalling pathway of Sp1 remains unclear. Our data showed that upregulation of Sp1 in the nucleus was abolished when podocytes were pre-treated with NAC or AFC, suggesting that ROS or p21Ras are involved in the translocation of Sp1. Unlike NF-κB, Sp1 could not be inhibited by PD98059. They explained why PD98059 partially blocked the CML-induced expression of MCP-1 mRNA. In fact, each of the transcription factors is very important during activation of the MCP-1 gene proximal promoter [43].

In conclusion, AGE and CML induce MCP-1 expression in podocytes via RAGE. Intracellular ROS are the central mediators in the RAGE signalling pathway. Both NF-λB and Sp1 are regulators of MCP-1 gene transcription. An inhibitor of the signalling pathway may raise the possibility of specific therapy to prevent macrophage-mediated diabetic injury of the kidney.

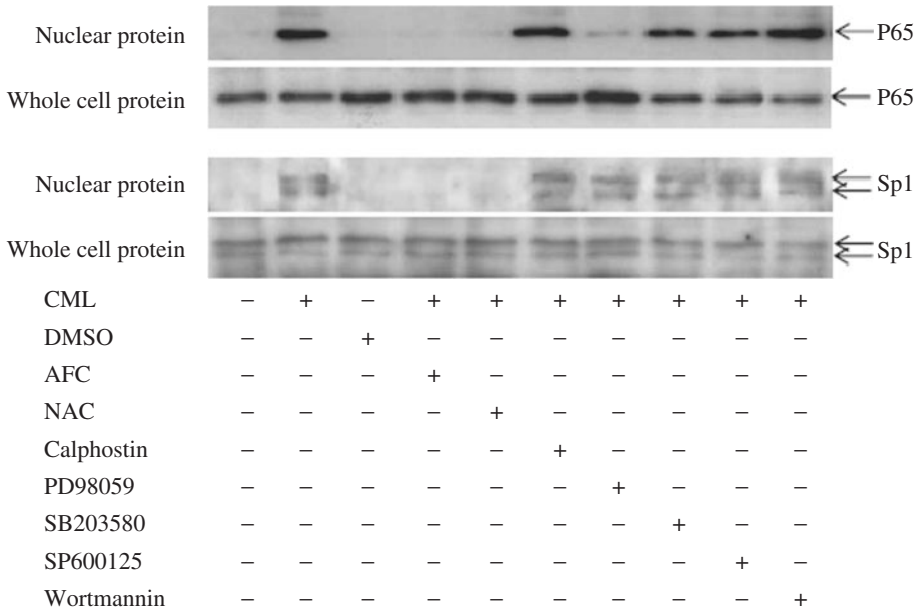

Fig. 10. Activation of NF-κB and Sp1 by CML was dependent on ROS and p21Ras. Podocytes were pre-treated with AFC (50 μM), NAC (30 mM), calphostin (100 nM), PD98059 (50 μM), SB203580 (10 μM), SP600125 (1 μM), wortmannin (100 nM) and DMSO (1:1000) for 30 min, then incubated with 500 μg/ml of CML for 120 min. Nuclear proteins and whole cell proteins were prepared, normalized to equal protein concentration and analysed by western blotting using antibodies to p65 and Sp1.

Acknowledgements. We thank Miss T. Shibata and M. Tamano for their excellent technical assistance. Dr Y. Suzuki provided invaluable suggestions throughout the course of this work.

Conflict of interest statement. None declared.

References

1. Prodjosudjadi W, Gerritsma JS, van Es LA, Daha MR, Bruijn JA. Monocyte chemoattractant protein-1 in normal and diseased human kidneys: an immunohistochemical analysis. *Clin Nephrol* 1995; 44: 148–155
2. Banba N, Nakamura T, Matsumura M, Kuroda H, Hattori Y, Kasai K. Possible relationship of monocyte chemoattractant protein-1 with diabetic nephropathy. *Kidney Int* 2000; 58: 684–690
3. Chow F, Ozols E, Nikolic-Paterson DJ, Atkins RC, Tesch GH. Macrophages in mouse type 2 diabetic nephropathy: correlation with diabetic state and progressive renal injury. *Kidney Int* 2004; 65: 116–128
4. Ha H, Yu MR, Choi YJ, Kitamura M, Lee HB. Role of high glucose-induced nuclear factor-kappaB activation in monocyte chemoattractant protein-1 expression by mesangial cells. *J Am Soc Nephrol* 2002; 13: 894–902
5. Yamagishi S, Inagaki Y, Okamoto T *et al*. Advanced glycation end product-inducted apoptosis and overexpression of vascular endothelial growth factor and monocyte chemoattractant protein-1 in human cultured mesangial cells. *J Biol Chem* 2002; 277: 20309–20315
6. Wendt TM, Tanji N, Guo J *et al*. RAGE drives the development of glomerulosclerosis and implicates podocytes activation in the pathogenesis of diabetic nephropathy. *Am J Pathol* 2003; 162: 1123–1137
7. Tanji N, Markowitz GS, Fu C *et al*. The expression of advanced glycation end-products and their cellular receptor RAGE in diabetic nephropathy and non-diabetic renal disease. *J Am Soc Nephrol* 2000; 11: 1656–1666
8. Schmidt AM, Vianna M, Gerlach M *et al*. Isolation and characterization of binding proteins for advanced glycosylation end products from lung tissue which are present on the endothelial cell surface. *J Biol Chem* 1992; 267: 14987–14997
9. Neeper M, Schmidt AM, Brett J *et al*. A cell surface receptor for advanced glycosylation end products of proteins. *J Biol Chem* 1992; 267: 14998–15004
10. Hofmann MA, Drury S, Fu C *et al*. RAGE mediates a novel proinflammatory axis: a central cell surface receptor for S100/calgranulin polypeptides. *Cell* 1999; 97: 889–901
11. Yamamoto Y, Kato I, Doi T *et al*. Development and prevention of advanced diabetic nephropathy in RAGE-overexpressing mice. *J Clin Invest* 2001; 108: 261–268
12. Schmidt AM, Yan SD, Yan SF, Stern DM. The multiligand receptor RAGE as a progression factor amplifying immune and inflammatory responses. *J Clin Invest* 2001; 108: 949–955
13. Lander HM, Tauras JM, Ogiste JS, Hori O, Moss RA, Schmidt AM. Activation of the receptor for advanced glycation end products triggers a p21(ras)-dependent mitogen-activated protein kinase pathway regulated by oxidant stress. *J Biol Chem* 1997; 272: 17810–17814.
14. Huttunen HJ, Fages C, Rauvala H. Receptor for advanced glycation end products (RAGE)-mediated neurite outgrowth and activation of NF-kappaB require the cytoplasmic domain of the receptor but different downstream signaling pathways. *J Biol Chem* 1999; 274: 19919–19924
15. Shaw SS, Schmidt AM, Banes AK, Wang X, Stern DM, Marrero MB. S100B-RAGE-mediated augmentation of angiotensin II-induced activation of JAK2 in vascular smooth muscle cells is dependent on PLD2. *Diabetes* 2003; 52: 2381–2388
16. Tanaka N, Yonekura H, Yamagishi S, Fujimori H, Yamamoto Y, Yamamoto H. The receptor for advanced glycation end products is induced by the glycation products themselves and tumour necrosis factor-alpha through nuclear factor-kappa B, and by 17 beta-estradiol through Sp1 in human vascular endothelial cells. *J Biol Chem* 2000; 275: 25781–25790

17. Bierhaus A, Schiekofer S, Schwaninger M *et al*. Diabetes-associated sustained activation of the transcription factor nuclear factor nuclear factor-kappaB. *Diabetes* 2001; 50: 2792–2808
18. Takeuchi M, Bucala R, Suzuki T *et al*. Neurotoxicity of advanced glycation end-products for cultured cortical neurons. *J Neuropathol Exp Neurol* 2000; 59: 1094–1105
19. Mundel P, Reiser J, Kriz W. Induction of differentiation in cultured rat and human podocytes. *J Am Soc Nephrol* 1997; 8: 697–705
20. Bass DA, Parce JW, Dechatedlet LR, Szejda P, Seeds MC, Thomas M. Flow cytometric studies of oxidative products formation by neutrophils: a graded response to membrane stimulation. *J Immunol* 1983; 130: 1910–1917
21. Bae YS, Kang SW, Seo MS *et al*. Epidermal growth factor (EGF)-induced generation of hydrogen peroxide. Role in EGF receptor-mediated tyrosine phosphorylation. *J Biol Chem* 1997; 272: 217–221
22. Doublier S, Salvidio G, Lupia E *et al*. Nephrin expression is reduced in human diabetic nephropathy: evidence for a distinct role for glycated albumin and angiotensin II. *Diabetes* 2003; 52: 1023–1030
23. Tryggvason K, Wartiovaara J. Molecular basis of glomerular permselectivity. *Curr Opin Nephrol Hypertens* 2001; 10: 543–549
24. Amann B, Tinzmann R, Angelkort B. ACE inhibitors improve diabetic nephropathy through suppression of renal MCP-1. *Diabetes Care* 2003; 26: 2421–2425
25. Wada T, Yokoyama H, Matsushima K, Kobayashi K. Monocyte chemoattractant protein-1: does it play a role in diabetic nephropathy? *Nephrol Dial Transplant* 2003; 18: 457–459
26. Viedt C, Dechend R, Fei J, Hansch GM, Kreuzer J, Orth SR. MCP-1 induces inflammatory activation of human tubular epithelial cells: involvement of the transcription factors, nuclear factor-κB and activating protein-1. *J Am Soc Nephrol* 2002; 13: 1534–1547
27. Cohen MP, Hud E. Measurement of plasma glycoalbumin levels with a monoclonal antibody-based ELISA. *J Immunol Methods* 1989; 122: 279–283
28. Abel M, Ritthaler U, Zhang Y *et al*. Expression of receptors for advanced glycosylated end products in renal disease. *Nephrol Dial Transplant* 1995; 10: 1662–1667
29. Yamazaki H, Saito A, Ooi H, Kobayashi N, Mundel P, Gejyo F. Differentiation-induced cultured podocytes express endocytically active megalin, aheymann nephritis antigen. *Nephron Exp Nephrol* 2004; 96: e52–e58
30. Greiber S, Muller B, Daemisch P, Pavenstadt H. Reactive oxygen species alter gene expression in podocytes: induction of granulocyte macrophage-colony-stimulating factor. *J Am Soc Nephrol* 2002; 13: 86–95
31. Kojima K, Matsui K, Nagase M. Protection of alpha(3) integrin-mediated podocyte shape by superoxide dismutase in the puromycin aminonucleoside nephrosis rat. *Am J Kidney Dis* 2000; 35: 1175–1185
32. Vega-Warner V, Ransom RF, Vincent AM, Brosius FC, Smover WE. Induction of antioxidant enzymes in murine podocytes precedes injury by puromycin aminonucleoside. *Kidney Int* 2004; 66: 1881–1889
33. Xu D, Kyriakis JM. Phosphatidylinositol 3′-kinase-dependent activation of renal mesangial cell Ki-Ras and ERK by advanced glycation end products. *J Biol Chem* 2003; 278: 39349–39355
34. Ping D, Jones PL, Boss JM. TNF regulates the *in vivo* occupancy of both distal and proximal regulatory regions of the MCP-1/JE gene. *Immunity* 1996; 4: 455–469
35. Ping D, Boekhoudt G, Zhang F *et al*. Sp1 binding is critical for promoter assembly and activation of the MCP-1gene by tumour necrosis factor. *J Biol Chem* 2000; 275: 1708–1714
36. Park SK, Yang WS, Han NJ *et al*. Dexamethasone regulates AP-1 to repress TNF-α induced MCP-1 production in human glomerular endothelial cells. *Nephrol Dial Transplant* 2004; 19: 312–319
37. Marchand P, Resch K, Radeke HH. Selective inhibition of monocyte chemoattractant protein-1 gene expression in human embryonal kidney cells by specific ripple helix-forming oligonucleotides. *J Immunol* 2000; 164: 2070–2076
38. Keembiyehetty CN, Candelaria RP, Majumdar G *et al*. Paradoxical regulation of Sp1 transcription factor by glucagons. *Endocrinology* 2002; 143: 1512–1520
39. Zhang X, Liu Y. Suppression of HGF receptor gene expression by oxidative stress is mediated through the interplay between Sp1 and Egr-1. *Am J Physiol* 2003; 284: F1216–F1225
40. Bontemps Y, Vuillermoz B, Antonicelli F *et al*. Specific protein-1 is a universal regulator of UDP-glucose dehydrogenase expression: its positive involvement in transforming growth factor-beta signaling and inhibition in hypoxia. *J Biol Chem* 2003; 278: 21566–21575
41. Benckert C, Jonas S, Cramer T *et al*. Transforming growth factor beta 1 stimulates vascular endothelial growth factor gene transcription in human cholangiocellular carcinoma cells. *Cancer Res* 2003; 63: 1083–1092
42. Silbiger S, Lei J, Ziyadeh FN, Neugarten J. Estradiol reverses TGF-beta1-stimulated type IV collagen gene transcription in murine mesangial cells. *Am J Physiol* 1998; 274: F1113–F1118
43. Boekhoudt GH, Guo Z, Beresford GW, Boss JM. Communication between NF-κB and Sp1 controls histone acetylation within the proximal promoter of the monocyte chemoattractant protein 1 gene. *J Immunol* 2003; 170: 4139–4147

Received for publication: 6.7.05
Accepted in revised form: 18.9.05